Matter

CellPress

Article

Swaying gel: chemo-mechanical self-oscillation based on dynamic buckling

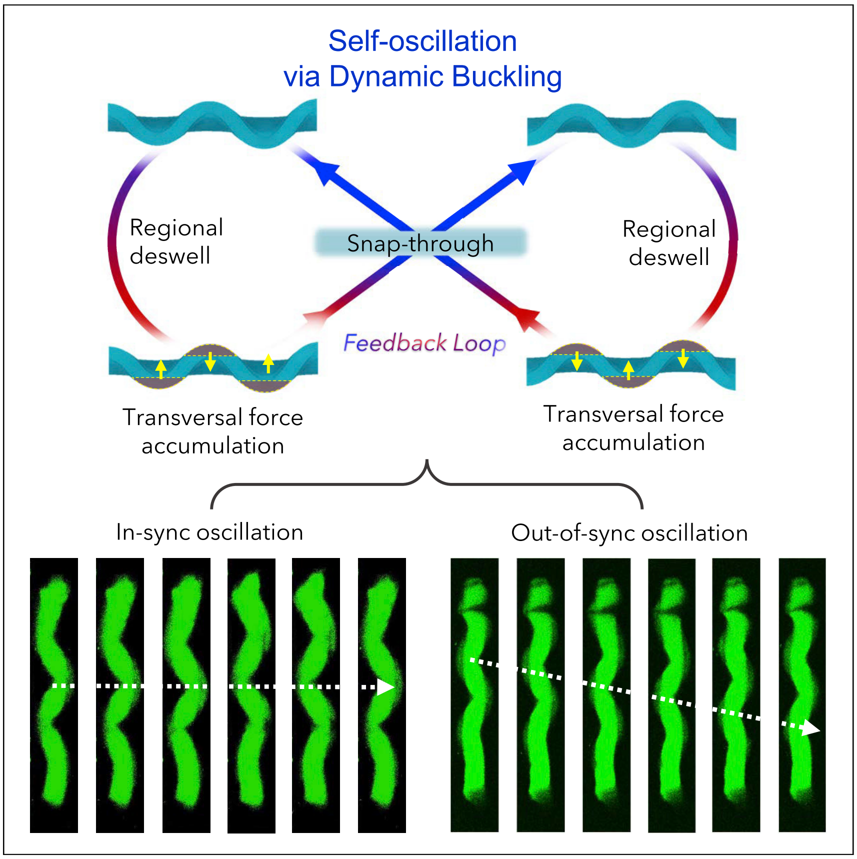

Buckling, or the sudden sideway deflection of structures under axial compressive stress, is a well-known classic mechanical instability phenomenon. By constructing a feedback loop to govern the reversible reconfiguration of a responsive hydrogel strip between bistable or multi-stable buckling configurations, an adaptable and modular self-oscillation system that does not require specific material or special chemistry was established.

Mutian Hua, Cheolgyu Kim, Yingjie Du, Dong Wu, Ruobing Bai, Ximin He

ximinhe@ucla.edu

HIGHLIGHTS

A generic design of dynamic buckling-based self-oscillation system

A transient-state multiphysics model for elucidating mechanism and design principles

For separation, robots, reaction modulation, energy harvest, and logistic devices

3 **Understanding**
Dependency and conditional studies on material behavior

Hua et al., Matter 4, 1–13
March 3, 2021 © 2021 Elsevier Inc.
https://doi.org/10.1016/j.matt.2021.01.002

Please cite this article in press as: Hua et al., Swaying gel: chemo-mechanical self-oscillation based on dynamic buckling, Matter (2021), https://doi.org/10.1016/j.matt.2021.01.002

Matter

CellPress

Article

Swaying gel: chemo-mechanical self-oscillation based on dynamic buckling

Mutian Hua,[1,3] Cheolgyu Kim,[1,3] Yingjie Du,[1] Dong Wu,[1] Ruobing Bai,[2] and Ximin He[1,4,*]

SUMMARY

Self-oscillating systems are powerful tools for transducing static energy inputs into repetitive motions without the aid of external control units. The challenge in sustaining the far-from-equilibrium motion of an oscillating material is to avoid the tendency of reaching thermodynamic equilibrium or get pinned at steady states in the dynamic process. While living organisms present elegant strategies in myriad self-oscillations (e.g., peristalsis, cilia motion, homeostasis), current synthetic self-oscillating systems often rely on a fast actuation/reaction, to maintain the far-from-equilibrium motion, which prescribe highly specific chemical reactions and a material microstructure with limited stimuli and movement modes. Here, we present a dynamic buckling-based design for creating self-oscillating systems. The oscillation arises from the self-driven snap-through of a responsive hydrogel between bi-/multi-stable buckling configurations governed by a feedback loop. With broad choices of materials, tunable mechanics, and physical simplicity, this system opens a new venue for unlimited autonomous-oscillating materials applications.

INTRODUCTION

Oscillations, repetitive variations in time, energy, or configuration, are ubiquitous and vital functions in nature, spanning from DNA replication, central pattern generators (CPGs) for breathing, to millions of modes of solar and star oscillations in the universe. In our daily life, human beings benefit from the alternating current in power distribution, thrusting heat engines in kinetic energy generation and many more mechanical oscillations for autonomic and intelligent systems. The elementary unit, the mechanical oscillator, typically relies on alternating input power and external modulation to stimulate or generate periodic spatiotemporal motions. Self-oscillators, by contrast, can uniquely harvest energy autonomously and generate sustained repetitive motion from static inputs by controlling the phase of external power that acts on it itself. Self-oscillating materials, with the rich dynamics and intriguing autonomy, have drawn great attention for fundamental science and applications.[1–10]

Creating self-oscillation is challenging, since all thermodynamic systems tend to reach equilibrium (with either maximum entropy or minimum free energy) or steady states (with constant energy input), known from classic thermodynamic theory. Hence, how to break the equilibrium or steady state of a process is the key to design of self-oscillators. Nature presents elegant ways to generate biological rhythms, i.e., CPGs by sequential rise and fall of two reciprocal neural stimulation through complex feedback pathways.[11,12] However, realizing such an alternating dominance of two opposite processes autonomously using synthetic materials is challenging. One of the first synthetic self-oscillating materials involves periodic volumetric

Progress and potential

Mechanical oscillations are one of the most rudimentary but important motions useful for energy conversion, autonomation, robotics, etc. Creating an oscillation is challenging, since all processes tend to reach equilibria or steady state. Hence, how to break the steady state of a process is the key challenge in self-oscillator design. This manuscript introduces a modular and adaptable design for a self-oscillating system applicable to various materials, which is achieved by a feedback loop-governed snap-through of a responsive hydrogel strip between bistable or multi-stable buckling configurations. A transient-state multiphysics model was also developed to elucidate the fundamental mechanism and established a broadly applicable designer model. Owing to the broad choices of materials, tunable mechanics, and physical simplicity, the introduced design has the potential to make transformative impacts on autonomous robots, separation, reaction modulation, and biomimetic designs.

Please cite this article in press as: Hua et al., Swaying gel: chemo-mechanical self-oscillation based on dynamic buckling, Matter (2021), https://doi.org/10.1016/j.matt.2021.01.002

expansion-contraction of a stimuli-responsive hydrogel driven by the self-oscillating Belousov-Zhabotinsky reaction (B-Z reaction), which opens an era for self-governed locomotion, object transport, etc.[4,5,7,8,13,14] The mechanical oscillation arises from the passive volumetric response of the thermal responsive hydrogel to the oscillating re-dox state of the metal ions in the classic B-Z reaction, where the oxidized state induces swelling and the reduced state induces shrinking of the material.[13] The rapid conversion from one state to the other via autocatalytic reactions (one of the products is a reactant) enables the alternating dominance of the forward and backward reaction,[15,16] which avoids pinning at the thermodynamic equilibrium, leading to this far-from-equilibrium chemistry and subsequent mechanical oscillation.[17,18] Another design of synthetic self-oscillators features flapping motions of cantilever-shaped light-responsive materials.[1,3,9] These out-of-equilibrium actuations arise from a self-shadowing-enabled negative feedback loop inherent in the dynamic light-material interactions, promoted by the fast and reversible shape change of the photoresponsive hydrogels or liquid crystal networks.[2,3,9] The rapidness in the shape changing is the prerequisite for creating distinct illumination-shading cycles for driving away from equilibrium, without which the cantilever would trap at the incident angle.[3,19]

Extracting the essential design principle of the aforementioned systems, a mechanically self-oscillating system generally consists of a rapidly and reversibly responsive material/reaction and two opposite stimuli (e.g., re-dox, illumination-shading), which act alternatingly on the material with a rhythm modulated by a negative feedback loop (e.g., the reaction products or material reconfiguration provide feedback and, in turn, serve as input for opposite reaction/configuration). Importantly, the rapidness of the actuation/reaction is essential and critical for initiating and maintaining the far-from-equilibrium states, to exhibit oscillation (e.g., exponential production rate of the autocatalytic reaction, fast bending of the high-response-rate polymer). Essentially, in these self-oscillating systems, the central positions of oscillation coincide with a thermodynamic steady state in which the material can remain static; meanwhile, a fast actuation/reaction helps to generate mechanical inertia for the material to overshoot beyond the equilibrium position or to generate chemical overshoots to an opposite chemical state for sustainable oscillation. Such a requirement of rapidness prescribes the demanded chemical reaction, material microstructure, and high thermal/mass diffusion, which has made the existing self-oscillating material systems highly specific with a small repertoire, and difficult to initiate other desirable properties (e.g., high mechanical strength) and functions (e.g., response to diverse stimuli, diverse movement modes). The desires for new and diverse self-oscillating systems call for a universal design that can break these limits. Specifically, to circumvent the requirement for inertia-driven overshooting, a new strategy for maintaining far-from-equilibrium oscillation is desirable.

Buckling, or the sudden sideway deflection of structures under axial compressive stress, is a classic mechanical instability phenomenon, and could also serve as a unique way to reconfigure materials.[20–25] While buckling has been extensively studied for decades, mostly in the (quasi)static or passive states, the dynamic and active changing of different buckling configurations under constant stimulation are still being actively exploited. In contrast to the continuous actuation of material in the reported self-oscillating systems, buckling of materials is slow during stress accumulation but rather abrupt during displacement (termed as ‘‘snap-through’’), presenting discrete buckling configurations. The transient intermediate state is thermodynamically unfavorable and thus does not stably exist. The transition between configurations is through rapid hopping between the discrete states that are

[1] Department of Material Science and Engineering, University of California Los Angeles, Los Angeles, CA 90095, USA

[2] Division of Engineering and Applied Science, California Institute of Technology, Pasadena, CA 91125, USA

[3] These authors contributed equally

[4] Lead contact

*Correspondence: ximinhe@ucla.edu

https://doi.org/10.1016/j.matt.2021.01.002

Please cite this article in press as: Hua et al., Swaying gel: chemo-mechanical self-oscillation based on dynamic buckling, Matter (2021), https://doi.org/10.1016/j.matt.2021.01.002

mechanically locked by the potential wells, making the system resistant to fluctuations of external input. With appropriate design of a feedback loop that reconfigures the material between the quantized configurations, the buckling phenomenon could serve as a new method for breaking the thermodynamic equilibria and creating reliable and highly repeatable oscillation.[3,26–28]

Here, we demonstrate a buckling-based design for sustained self-oscillating systems, which possesses a bistable state with a double-well structure of potential energy to define the two oscillation maxima. Placed in between two chemically distinct environments, the constrained reversibly responsive material, initially dominated by the swelling-inducing stimulus in its relaxed state, swells and eventually buckles to release the accumulated stress. Such a buckled configuration, in turn, causes the material to be dominated by the deswelling-inducing stimulus instead and consequently de-swells to relax. The material autonomously sways between two complementary buckling configurations repetitively, thus exhibiting self-oscillation (Figure 1A). Uniquely, the mechanically static steady state is easily broken owing to the continuous snap-through between the discrete conformations even without rapid actuation. We have demonstrated the tunability of the oscillation behavior (amplitude and period) and the corresponding operation windows by changing the volume expansion ratio and rate of the material. Through finite element modeling, we have established a model that validates the underlying mechanism of this unique dynamic buckling and predicts the oscillation pattern of the system. Ultimately, we have showcased the universality and modular design of this self-oscillating system by successfully generating sustained oscillation using different stimuli with the same design principle. Owing to the broad choices of materials, tunable mechanics, and physical simplicity, the self-oscillating system has a broad-based platform, with potential to make transformative impacts on autonomous robots,[7,14,29–31] autonomous separation,[32] reaction modulation,[33] autonomous mechanical metamaterials, energy harvesting,[34] mechano-logistic devices,[26,27] sensing,[35] and biomimetic designs.[36]

RESULTS AND DISCUSSION

Sustained oscillation by dynamic buckling

The typical customizable setup is illustrated in Figure 1A. A strip of stimuli-responsive hydrogel (dimensions, 150 μm [W] × 250 μm [H] × 2.6 mm [L]) is covalently anchored to a rigid glass substrate at the bottom of a microfluidic channel (Figure S1). When the confined slender hydrogel is swelled, the bottom constraint generates an axial compressive force, which provides the buckling condition for the hydrogel strip. To construct the feedback pathway, we formed a spatially distinct dual-stimuli environment around the hydrogel by an upper-lower laminar flow of two liquid layers (upper, swelling solution; lower, deswelling solution, Figure S2). The top surface of the relaxed hydrogel extrudes into the upper-layer stimuli but will exit the upper layer when buckled. When the upper-layer stimuli strongly induce swelling/buckling of the hydrogel while the lower layer induces deswelling/un-buckling of the hydrogel, a negative feedback loop could be constructed, such that the material tends to buckle when in its unbuckled configuration and tends to un-buckle when in its buckled configuration, resulting in an interesting swaying behavior.

Using this design, we first demonstrated the self-oscillation stimulated by simple acid and base stimuli. A pH-responsive hydrogel poly(acrylamide-co-acrylic acid) (p(AAm-co-AAc)) was used as the stimuli-responsive material for fabricating the gel strip. The electrolyte hydrogel (pK_a = 4.3) swells when immersed in solution of

Please cite this article in press as: Hua et al., Swaying gel: chemo-mechanical self-oscillation based on dynamic buckling, Matter (2021), https://doi.org/10.1016/j.matt.2021.01.002

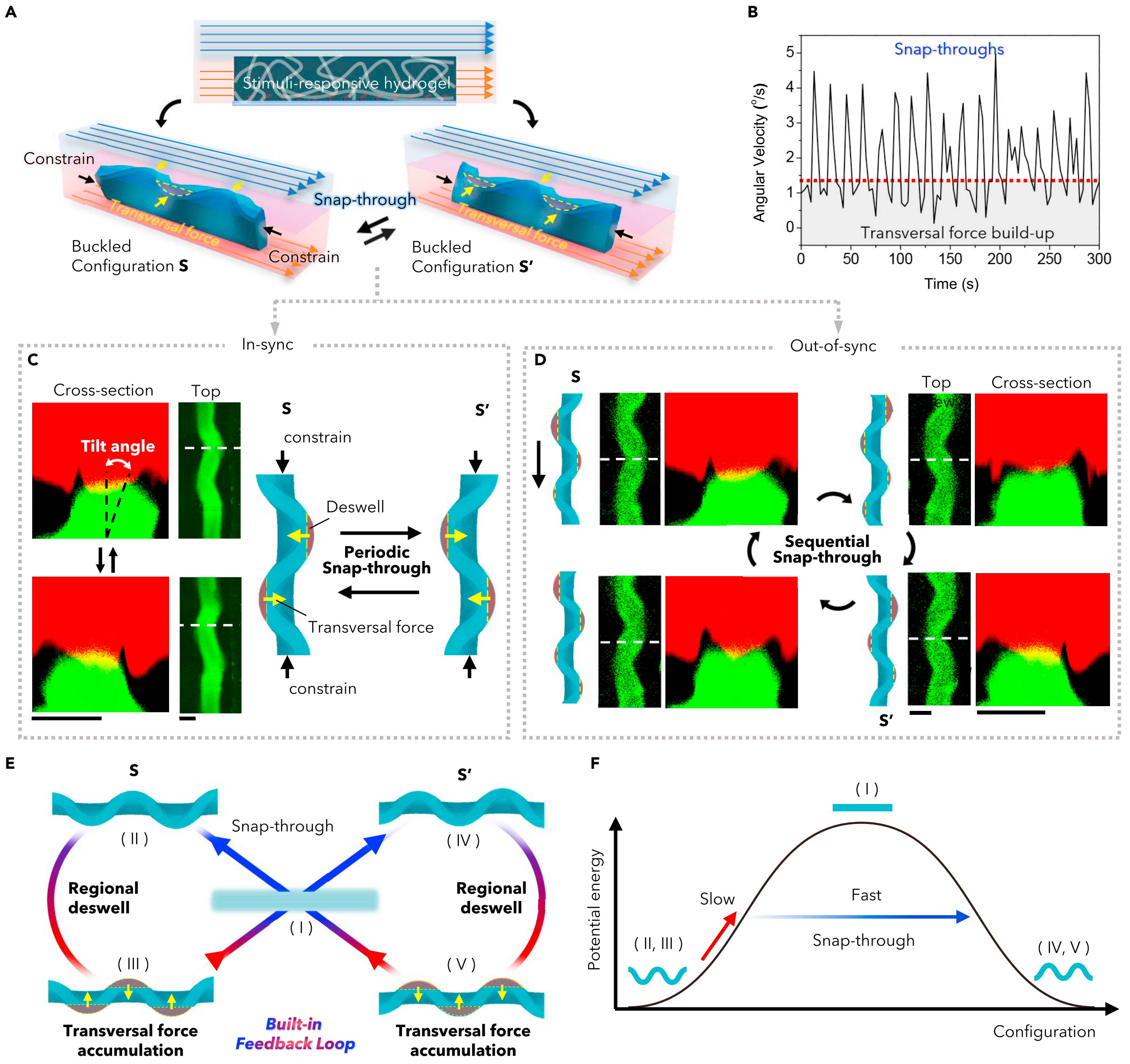

Figure 1. Dynamic buckling of a hydrogel strip via formation of in-sync/out-of-sync oscillations

(A) Schematic showing the oscillation of the hydrogel strip between two complementary buckled configurations in a dual-stimuli environment. The upper layer (light blue) is the flow of swelling-inducing stimuli and the lower layer (pink) is the flow of deswelling-inducing stimuli.

(B) Angular velocity of the cross-section of a peak section of the gel strip during oscillation, showing the typical characteristic of snap-through (Video S1).

(C) Confocal microscopy images of the oscillating hydrogel strip in the in-sync mode. The schematic shows the buildup of the transversal force that facilitates the snap-through.

(D) Confocal microscopy images of the oscillating hydrogel strip in the out-of-sync mode. The schematic shows the asynchronized buildup of transversal force. For the confocal images in (C and D), the hydrogel is colored in green, the alkaline solution in red, and the acidic solution in black. Scale bars, 200 μm.

(E and F) (E) Schematic of the oscillation process governed by the negative feedback loop arising from dynamic buckling via snap-through and (F) the corresponding potential energy diagram.

pH > 4.3, due to deprotonation of the carboxylated polymer chain, and contracts in solution of pH < 4.3 due to protonation. A constant laminar flow of two pH-distinct streams (upper, NaOH solution [pH 13], 6–30 mL/h; lower, HCl solution [pH 2],

Please cite this article in press as: Hua et al., Swaying gel: chemo-mechanical self-oscillation based on dynamic buckling, Matter (2021), https://doi.org/10.1016/j.matt.2021.01.002

2–10 mL/h) was used as the stimuli input. This setup successfully perturbed the buckling of the hydrogel into a dynamic and reversible process that shows sustained oscillation characteristics. The hydrogel either bistably swayed between two complementary configurations (in-sync, Figure 1C) or dynamically undulated between multi-stable configurations (out-of-sync, Figure 1D).

The in-sync oscillation (Figure 1C) took place under relatively high flow rates (upper, NaOH solution [pH 13], 30 mL/h; lower, HCl solution [pH 2], 10 mL/h). The constrained pH-responsive hydrogel strip, which initially extruded into the swelling-inducing alkaline layer, first swelled to attain a buckled configuration "S" (Figure 1C, right). Clearly viewed from the cross-sections of a peak/valley section of the strip (Figure 1C, left), the gel tilted significantly, which led the valley/peak region of the top surface (marked by a crescent shape in Figure 1C, right) to disengage from the alkaline layer and enter the deswelling-inducing acidic layer. This crescent-shaped region then locally de-swelled, which generated the transversal force in the direction opposite to the current tilting direction, for the onset of snap-through. At this moment, however, the nodes between valleys and peaks still remained swollen, which maintained the axial compression in the gel strip, i.e., the buckling-favorable condition. This local deswelling-generated transversal force, when accumulated and exceeded the snap-through threshold, suddenly activated and pushed this globally swollen but longitudinally compressed gel strip to the opposite direction. As all peak and valley regions switch at once, the strip rapidly jumped from configuration S to its complementary configuration S′ (Figure 1C, right). Once entering the complementary buckling configuration, the mirroring process for the backward snap-through takes place. As this process is repeated cyclically, the hydrogel strip self-oscillates between two opposite buckling configurations S and S′ (Video S1).

The time-lapse angular velocity of the swaying gel at a fixed cross-section (Figure 1B; Video S2) shows periodic peaks, which correspond to and verified the rapid transient snap-through moments; the moments when the convex-concave inter-transformation occurs, triggered by the perturbation from the external transversal force. Essentially, the oscillation pathway of the hydrogel strip is governed by the buckling-modulated feedback (Figures 1E and S3), corresponding to the energy states as depicted in Figure 1F. The gel strip started from the energetically unfavorable unbuckled configuration (I), where the top surface was continuously swelling. To release the swelling-induced stress due to the constraints, the strip buckled to the configuration S for energy minimization (I → II). This, in turn, led to regional deswelling and a buildup of transversal force for snap-through, while this configuration is locked by a thermodynamic tendency to minimize energy (II → III). As the local deswelling of gel strip continued to provide activation energy until above the energy barrier between S and S′, the gel strip snaps through the high-tension, neutral position and rapidly transforms to the opposite buckled configuration S′ (III → IV). This again initiates the onset of the reverse snap-through from configuration S′ back to S (IV → V → II), the next round of the cycle, and so on, along this dynamic buckling-based feedback loop.

To identify the essential conditions for the oscillation to occur, we conducted two control experiments under the identical setup to understand the importance of (1) the buckling condition and (2) the two opposite stimuli, respectively. First, we tested, using a hydrogel strip with a smaller height-to-width ratio (150 μm [H] × 200 μm [W]; geometrically unfavorable to buckle when swelled). As the top surface was still immersed in the upper swelling stimuli, the gel strip still swelled but did not buckle, nor could it oscillate (Video S3). This result proved that, despite having the condition to provide feedback with the two opposite stimuli, without the buckling-favorable condition the material tends to be pinned at the interface of the two opposite stimuli, as the slow and gradual swelling and deswelling processes reach steady state at the interface. Second, to understand the importance of the condition for enabling the generation and buildup of the transversal force, we tested the same gel strip under the same flow rate in the swelling alkaline solution only. In the absence of the deswelling stimuli, the gel buckled but remained in the same configuration (Video S4). This classic static bucking behavior proved the necessity of the two opposite stimuli to form the negative feedback loop. This also indicated that the shear force from flow could not generate the oscillation either.

Interestingly, a traveling wave-like, out-of-sync oscillation, based on the same mechanism, was observed under relatively low flow rates (upper, NaOH solution [pH 13], 6 mL/h; lower, HCl solution [pH 2], 2 mL/h). In the slower flow, the two stimuli layers inter-diffused and created a pH gradient on the gel surface (Figure S4). Correspondingly, along the longitudinal direction, the gel strip has gradient (de)swelling rates and thus gradient transversal-force-accumulation rates (marked by the size gradient of the crescent regions in Figure 1D). As a result, the peaks/valleys along the buckled hydrogel strip reached the snap-through threshold in succession (Video S5). Therefore, the S ↔ S′ transitions of different segments along the strip occurred non-simultaneously, rather than sequentially. With such a cascade of snap-throughs, the gel strip oscillated between the multi-stable configurations as a traveling wave (Figure 1D).

Mechanistic study of snap-through-driven self-oscillation

The above intriguing complex in-sync/out-of-sync oscillations presented a wealth of dynamics. It is important to obtain a clear mechanistic understanding for establishing a general design principle for the self-oscillation system and owning the prediction capabilities of the oscillating behaviors for broader applications. Here, we established a multiphysics model via dynamic finite element analyses (FEA) to study the mechanism of the dynamic buckling theoretically, with the transient states well captured and proofed. We first studied the in-sync oscillation. To alleviate the computational complexity, a spatially uniform chemical potential was applied to the top surface of a swollen and buckled hydrogel model, despite the fact that, in experiments, the top surface had certain spatial variations in chemical potential, as each section of the top surface partitioned slightly differently between the alkaline and acidic streams. By cyclically switching the applied chemical potential to swell and de-swell the gel model, we mimicked the alternating acidic and alkaline stimuli experienced by the hydrogel dynamically, and successfully captured the in-sync oscillation, which well matched the experimental results both configurationally and kinetically (Figures 2A and 2C; Video S6). The FEA model clearly visualized the stress distribution across the gel strip spatiotemporally in three dimensions, which verified the above hypothesized oscillation principle. The gradient of the X axis stress mapping of the hydrogel at its fully buckled state (Figure 2E) clearly represented the transversal force at the valley/peak region (previously marked by the crescent shape in Figure 1) that drove the snap-through in this material system. The stress mapping of the hydrogel at the transient moment passing through the central position showed that the stress was not fully relaxed (Figure 2F), which visualized and indicated that the condition for the onset of buckling is maintained even when the hydrogel transiently assumes the unbuckled configuration during the snap-through process. The simulation verified that, two opposite stimuli that act alternatingly on a reversibly responsive material, and using dynamic buckling for breaking

Please cite this article in press as: Hua et al., Swaying gel: chemo-mechanical self-oscillation based on dynamic buckling, Matter (2021), https://doi.org/10.1016/j.matt.2021.01.002

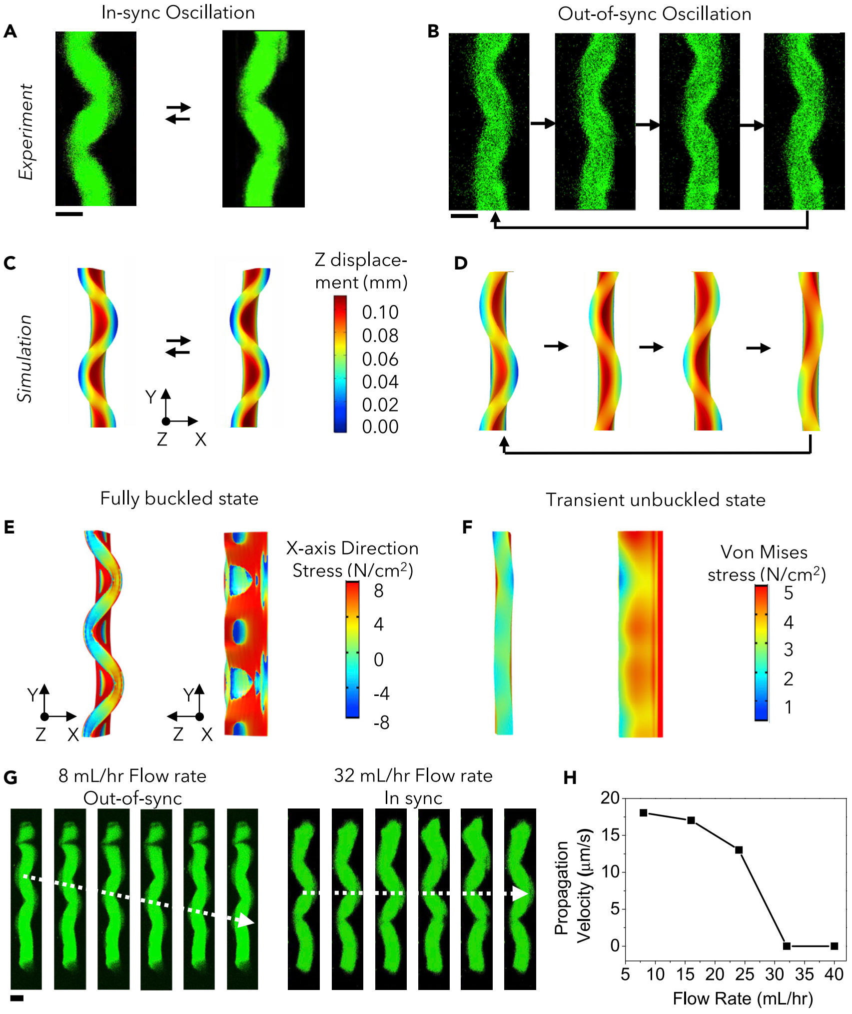

Figure 2. Mechanistic study of in-sync and out-of-sync oscillation

(A and B) An X-Y plane confocal microscopy image of the hydrogel strip in (A) in-sync oscillation and (B) out-of-sync oscillation, respectively.

(C and D) Z displacement mapping of the FEA hydrogel model in (C) in-sync oscillation and (D) out-of-sync oscillation, respectively.

(E) X axis stress mapping of the FEA model in fully buckled configuration.

(F) Von Mises stress mapping of the FEA model in transient unbuckled configuration.

(G) Time-lapse snapshots of the hydrogel strip under X-Y plane confocal microscopy under slow and fast flow rates.

(H) Peak/valley propagation velocity with respect to flow rate, showing the transition from out-of-sync mode to in-sync oscillation. Scale bars, 200 μm.

thermodynamic steady state, are essential and sufficient for generating mechanical self-oscillation.

To verify the mechanistic similarity between the out-of-sync and in-sync oscillations, we only added an additional chemical potential gradient from one end to the other end of the top surface of hydrogel strip to mimic the gradient stimuli concentration when simulating the out-of-sync oscillations (Figures S5 and S6). A similar undulation was obtained in the model under the applied conditions (Figures 2B and 2D; Video S7), which indicates that the out-of-sync oscillation shares the same mechanism with the in-sync oscillation and only differs by the asynchronized snap-throughs caused

Please cite this article in press as: Hua et al., Swaying gel: chemo-mechanical self-oscillation based on dynamic buckling, Matter (2021), https://doi.org/10.1016/j.matt.2021.01.002

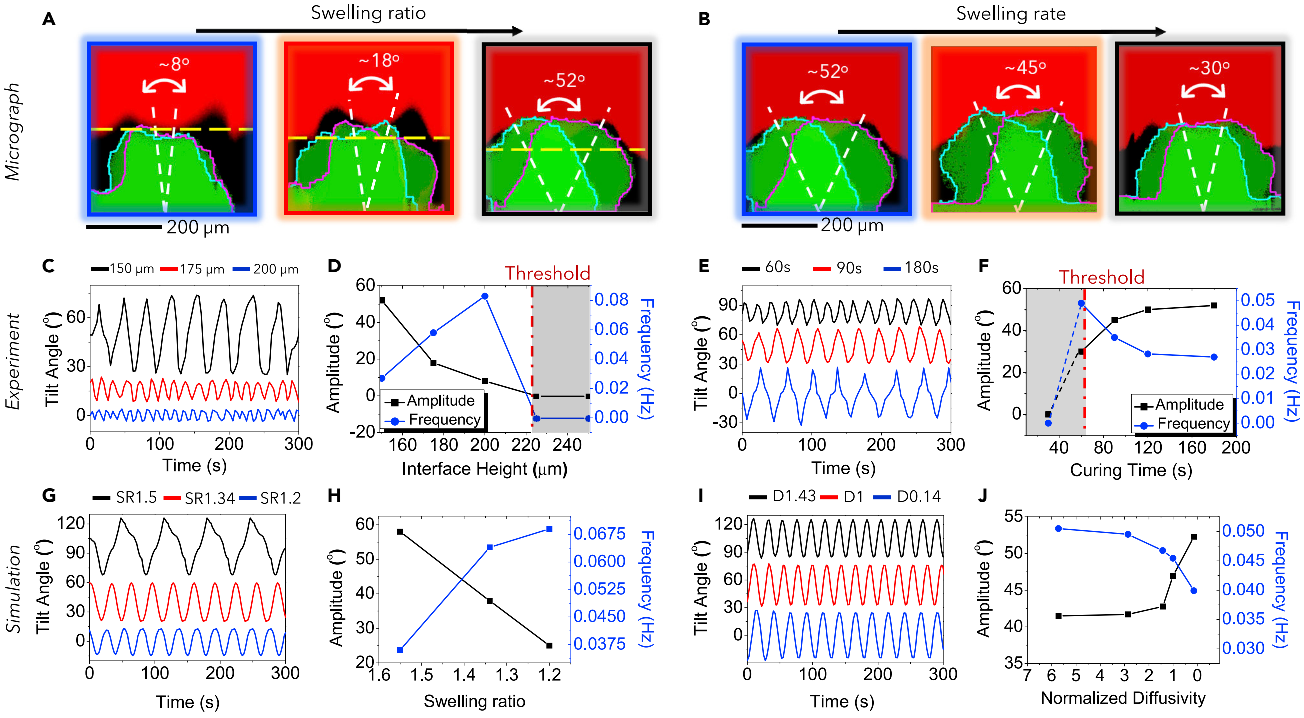

Figure 3. Tunable oscillation frequency and amplitude controlled by swelling ratio and rate

(A and B) Superimposed X-Z plane confocal images of the fully buckled configurations.

(C and E) Time-dependent tilting angle of the hydrogel shown in (A) and (B), respectively. (C) The bilayer interface height measured from the bottom of the hydrogel strip. (E) The curing time of the hydrogel strip.

(D and F) Oscillation amplitude and frequency trend as the function of interface height and curing time, respectively.

(G and I) FEA-simulated time-dependent tilting angle by varying the assigned hydrogel swelling ratio and diffusivity. (G) The swelling ratio assigned to the hydrogel model. (I) The diffusivity assigned to the hydrogel model.

(H and J) FEA-simulated oscillation amplitude and frequency trend with respect to the hydrogel swelling ratio and diffusivity. Scale bars, 200 μm.

by the chemical gradient. To further validate this point, we progressively increased the total flow rate from 8 to 40 mL/h while maintaining the upper:lower flow ratio at 3 (Figures 2G and 2H). Experimentally, we found that, with the increase of flow rate, the snap-through of the peaks/valleys became more synchronized as indicated by the decreasing peak/valley propagation velocity. When the total flow rate reached 32 mL/h in our setup, the peak/valley propagation velocity turned to zero, indicating the full transition from the out-of-sync oscillation to the in-sync oscillation (Figure 2H). Thus, it is confirmed that both oscillations share the same mechanism. Detailed modeling methods and parameters are described in the Supplemental Experimental Procedures and Table S1.

Programming and predicting self-oscillation patterns

Controlling and predicting the oscillation patterns for tailoring to specific locomotion demands is important for the application of self-oscillation systems. This requires identifying the governing parameters. Here, we have demonstrated the tunable oscillation frequency and amplitude by altering the bilayer interface position (determining swelling ratio) and the pore size of the hydrogel (determining swelling rate) and verified the oscillation patterns using the developed FEA model. In this part, we used 8 mL/h total flow rate for all experiments, which corresponded to the out-of-sync oscillation. Figure 3A shows the superimposed snapshots of a fixed cross-section in the central region of the hydrogel strip with an increasing upper-lower flow ratio. Consequently, the bilayer interface height was reduced, which

Please cite this article in press as: Hua et al., Swaying gel: chemo-mechanical self-oscillation based on dynamic buckling, Matter (2021), https://doi.org/10.1016/j.matt.2021.01.002

led to an increasing swelling ratio of the hydrogel strip, and thus a larger oscillation amplitude, as lower bilayer interface height allowed for longer contact time between the hydrogel and the swelling stimuli before the peaks/valleys of hydrogel strip were tilted enough to exit the upper layer. Meanwhile, a larger swelling ratio prescribes longer swelling times of the hydrogel under the same swelling rate. Therefore, a longer oscillation period is associated with larger oscillation amplitude, as graphically and statistically shown in Figures 3A, 3C, and 3D. The oscillation exists as long as the buckling condition is met; when raising the interface height beyond the height of the hydrogel, the oscillation disappeared, as the hydrogel strip was not swollen enough to enter the buckling-favorable condition. With the developed FEA model, we have obtained the same trend, in which the oscillation amplitude increases and the frequency decreases when an increasing swelling factor was assigned to the model.

Figure 3B shows superimposed snapshots of a fixed cross-section of the hydrogel strip with reducing curing time, hence increasing ionic diffusivity and response rate due to the increasing pore size (Figures S7 and S8). By increasing the response rate of the hydrogel, the buildup speed of the transversal force was increased, which allowed for more frequent snap-throughs, as the snap-through threshold could be reached at a less buckled state. As shown in Figures 3B, 3E, and 3F, the oscillation amplitude decreased with decreased curing time, accompanied by increases in frequency. The existence of the oscillation also required the buckling of the material (Figures S9 and S10). When the curing time was lower than 45 s, the hydrogel could not buckle due to the poor mechanical properties of the under-cured hydrogel (Figure S8) and thus did not show oscillation. By assigning higher diffusivity parameters in the FEA model, a similar trend was obtained (Figures 3I and 3J).

We further studied the effects of the total flow rate and the pH difference between the upper and lower layers on the oscillation patterns. In Figures 2G and 2H, we show that high flow rates (total flow >32 mL/h) resulted in the dynamic buckling changing from the out-of-sync mode to the in-sync mode. For low flow rates, decreasing the rate from 4 to 0.5 mL/h progressively dampened the oscillation (Video S8). This is because the strong inter-layer diffusion reduced the pH difference between the two layers, and thus the swelling and shrinking ability of the upper and lower layers were both significantly reduced. Ultimately, the oscillation stopped, and the buckling transitioned from the dynamic mode to the static mode at very low flow rates (0.5 mL/h). Reducing the pH difference showed similar effects on the oscillation (Video S9). The oscillation frequency reduced with smaller pH differences between the upper and lower layers (Figure S11). At extreme cases, the hydrogel showed static buckling instead of dynamic buckling, similar to the case of alkaline-only flow shown in Video S4.

Modular design for diverse applications

The controllable motion of the presented self-oscillation system set forth new designs for autonomous and programmable molecule/bio-separation, cargo transport, robotics, mechano-logic devices, microfluidic functions, and unlimited functions that arise from oscillation. Here, we demonstrated the pumping of sedimented particles inside a microfluidic channel (Figures 4A and 4B). Utilizing the undulating out-of-sync oscillation, the hydrogel strip shows superior particle-transporting speeds (up to 20 μm/s) and power (particle size >100 μm) to efficiently unclog the channel. The pumping of sedimented particles is fully autonomous without external intervention as the hydrogel strip self-oscillates in response to the steadily flowing fluid. Such transporting could also happen between upper and lower streams for

Please cite this article in press as: Hua et al., Swaying gel: chemo-mechanical self-oscillation based on dynamic buckling, Matter (2021), https://doi.org/10.1016/j.matt.2021.01.002

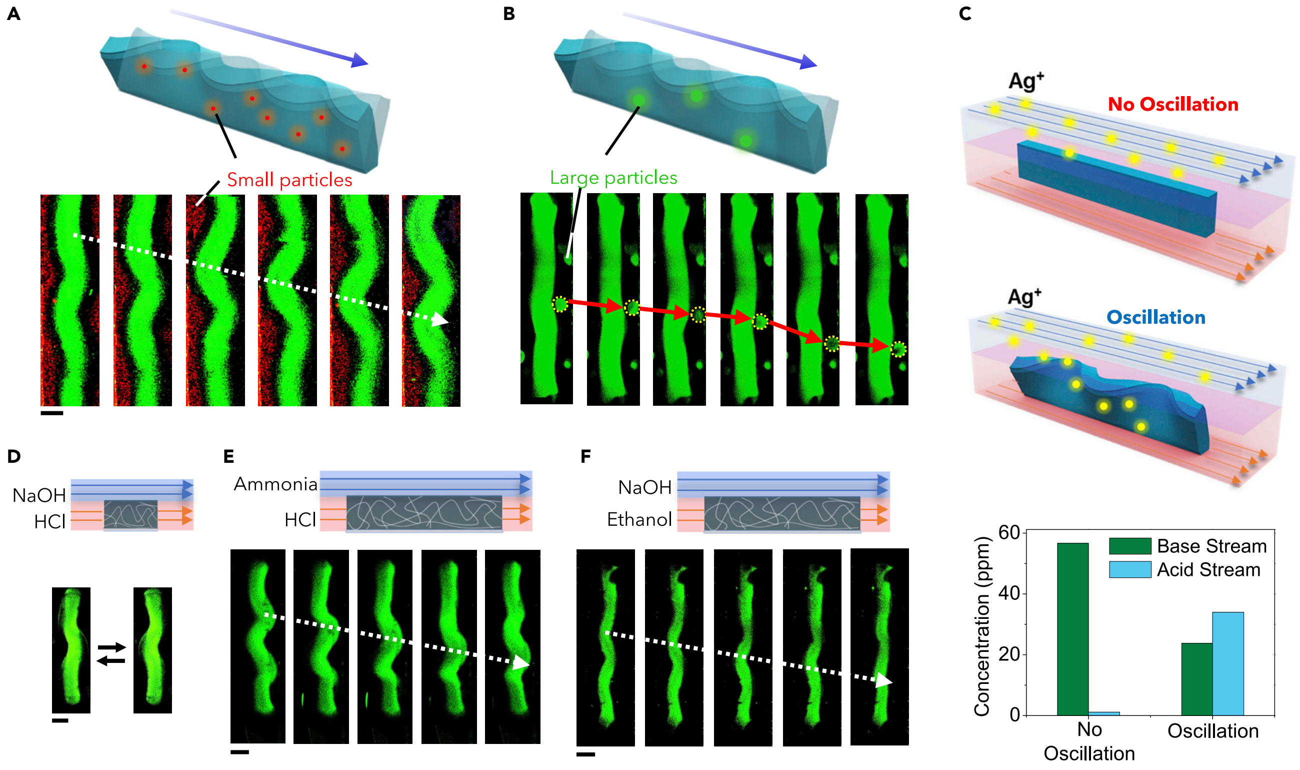

Figure 4. Universal and modular design of the proposed self-oscillation mechanism

(A and B) Autonomous pumping of (A) 10-µm fluorescent styrene particles and (B) 100-µm fluorescent acrylic particles.

(C) Molecule transportation between two laminar fluid streams; the upper base stream favors Ag^+ binding and the lower acid layer favors Ag^+ dissociation.

(D–F) (D) In-sync-only oscillation of a short p(AAm-co-AAc) hydrogel trip under NaOH-HCl stimuli. Out-of-sync oscillation of p(AAm-co-AAc) hydrogel (E) under ammonia-HCl stimuli and (F) under NaOH-80% ethanol stimuli. Scale bars, 200 µm.

applications, such as autonomous molecular separation or mixing. As shown in Figure 4C, the upper laminar stream is a basic fluid of Ag^+ with excess ammonia in the form of $[Ag(NH_3)_2]^+$, while the lower laminar stream is an acid fluid of dilute nitric acid. Using p(AAm-co-AAc) as the hydrogel strip, the $[Ag(NH_3)_2]^+$ adsorbs onto the hydrogel strip in the upper stream by binding to carboxyl groups, and dissociates in the lower stream as Ag^+ as the hydrogel moves from the upper stream to the lower stream during the oscillation. Without self-oscillation, the lower stream showed zero silver concentration. After the self-oscillation is switched on, the lower stream shows a high silver concentration of Ag^+.

The presented self-oscillation system features a universal and modular design which can be modified to different geometries and stimuli pairs. We tested the oscillation with hydrogel strips of different lengths; when the length of the gel is reduced to a single wavelength, in-sync mode will always take place (Figure 4D; Video S10), and when the gel becomes too short, oscillation disappears because the geometry no longer satisfies the buckling condition. Controllable regional oscillation was also achieved by changing the flow ratio of the upper- and lower-layer stimuli (Figure S12; Video S11). For demonstrating oscillations with different stimuli, we switched from HCl-NaOH stimuli to HCl-ammonia stimuli and HCl-ethanol stimuli. In both cases, oscillation was achieved (Figures 4D and 4E; Videos S12 and S13). It is noted that, in the latter case with ethanol, the deswelling mechanism is purely a physical reaction. The hydrogel strip shrinks dramatically in the presence of ethanol and is

Please cite this article in press as: Hua et al., Swaying gel: chemo-mechanical self-oscillation based on dynamic buckling, Matter (2021), https://doi.org/10.1016/j.matt.2021.01.002

relatively narrower in width compared with previous demonstrations because ethanol is a poor solvent for the hydrogel. The results demonstrate that the modular design of this dynamic-buckling-based self-oscillation system has the potential to function under various geometries and broad choices of chemical and physical stimuli.

Conclusion and perspective

In this work, a universal and modular design for a self-oscillation system has been demonstrated based on the dynamic buckling of a responsive material. The essential components for the presented self-oscillating system were a reversibly responsive material, an opposite stimuli pair, a feedback loop, and the onset of buckling. Fundamentally, the dynamic buckling resulted from the continuous buildup of transversal force induced by the buckling itself, guided by a built-in feedback loop that enabled the autonomous oscillation. The oscillation behavior is principally modulated by the volume change ratio and rate of the material. The numerical model developed in this study can serve as a design tool for new systems and to predict the oscillation behavior by changing input parameters. This customizable self-oscillation system design principle presents a potential broad impact with the demonstrated excellent versatility with physical simplicity, chemical amiability, and mechanical tunability. It is anticipated that it will open new avenues for autonomous robots, energy harvesting, bistable actuators, signal generators, mechano-logics and intelligent separation, and transport technology.

EXPERIMENTAL PROCEDURES

Resource availability

Lead contact

Further information and requests for resources and reagents should be directed to and will be fulfilled by the Lead contact, Ximin He (ximinhe@ucla.edu).

Materials availability

This study did not generate new unique reagents. Acrylamide and acrylic acid were purchased from Fisher Scientific. *N*,*N*′-Methylenebisacrylamide (Bis), 2-hydroxy-4′-(2-hydroxyethoxy)-2-methylpropiophenone (Irgacure 2959), 3-(trimethoxysilyl)propyl methacrylate (TMSPMA) fluorescein sodium salt were purchased from Sigma-Aldrich. Nile blue acrylamide was purchased from Polysciences. Polydimethylsiloxane (PDMS) prepolymer (Sylgard 184 Silicone Elastomer kits) was purchased from Ellsworth. Double-sided adhesive sheets (80 μm thickness) were purchased from Artgrafix. Polyethylene tubing (0.015 in [inner diameter] × 0.043 in [outer diameter]) was purchased from Fisher Scientific. All chemicals were used as purchased without further treatment.

Data and code availability

All data needed to evaluate the conclusions in the paper are present in the paper and/or Supplemental information. Additional data related to this paper may be requested from the authors.

Fabrication of hydrogel strips

The poly(acrylamide-co-acrylic acid) hydrogel precursor was prepared using 13 wt % acrylamide, 7 wt % acrylic acid, 1 wt % Bis, 1 wt % Irgacure 2959, and 0.1 wt % Nile blue acrylamide in deionized water. The hydrogel precursor was injected into a PDMS mold (dimensions, 150 μm [W] × 250 μm [H] × 2.6 mm [(L]) and covered by a TMSPMA-treated glass slide and UV cured for 180 s using a Dymax 5000-EC UV

Please cite this article in press as: Hua et al., Swaying gel: chemo-mechanical self-oscillation based on dynamic buckling, Matter (2021), https://doi.org/10.1016/j.matt.2021.01.002

flooding lamp. The PDMS mold was carefully lifted leaving the cured hydrogel strip attached to the treated glass slide. The hydrogel strip was then soaked in deionized water for 1 h and dried in ambient environment.

Fabrication of microfluidic device

The microfluidic channels comprise two layers. The pattern of both layers was designed with a channel width of 600 μm. The middle part of the channel has a channel length of 6 mm. The microfluidic channels for both layers were cut from three layers of double-sided adhesive sheets stacked together using a Universal Laser Systems PLS6MW laser cutter. Each layer of the microfluidic channel is 240 μm in thickness. The two layers of double-sided adhesive were carefully placed on the glass slide with hydrogel strip. The two layers were carefully aligned leaving the hydrogel strip in the center of the channel, and finally sealed by PDMS slabs (with pre-punctured holes at the inlet and outlet positions) as illustrated in Figure S1.

Characterization

Confocal microscopy was used for all recordings of the dynamic buckling of the hydrogel strips using a Leica DMi8 confocal microscope. The SEM images of the pore size of the p(AAm-co-AAc) hydrogel prepared using different curing time were taken using a Zeiss Supra 40VP SEM. The mechanical properties of the hydrogels were characterized using a TA DMA 850 machine. Dog-bone specimens (gauge length, 10 mm; gauge width, 2 mm; thickness, 1 mm) of the p(AAm-co-AAc) hydrogels with different curing times were prepared for measurement of the modulus of the hydrogels.

SUPPLEMENTAL INFORMATION

Supplemental information can be found online at https://doi.org/10.1016/j.matt.2021.01.002.

ACKNOWLEDGMENTS

This work was supported by the NSF Career award 1724526, AFOSR awards FA9550-17-1-0311, FA9550-18-1-0449 and FA9550-20-1-0344, and ONR awards N000141712117 and N00014-18-1-2314, the Hellman Fellows Funds, and the UCLA Faculty Career Development award from the University of California, Los Angeles.

AUTHOR CONTRIBUTIONS

X.H. conceived the concept, planned the project, and supervised the research. X.H. and M.H. designed and conducted the experiments and data analysis. M.H. and C.K. developed the model and numerical code and carried out the computational simulations. M.H., X.H., and C.K. wrote the initial draft. All authors participated in the discussion of the manuscript.

DECLARATION OF INTERESTS

The authors declare no competing interests.

Received: November 8, 2020
Revised: December 21, 2020
Accepted: December 31, 2020
Published: January 28, 2021

Please cite this article in press as: Hua et al., Swaying gel: chemo-mechanical self-oscillation based on dynamic buckling, Matter (2021), https://doi.org/10.1016/j.matt.2021.01.002

REFERENCES

1. Kumar, K., Knie, C., Bléger, D., Peletier, M.A., Friedrich, H., Hecht, S., Broer, D.J., Debije, M.G., and Schenning, A.P.H.J. (2016). A chaotic self-oscillating sunlight-driven polymer actuator. Nat. Commun. *7*, 1–8.
2. Gelebart, A.H., Vantomme, G., Meijer, E.W., and Broer, D.J. (2017). Mastering the photothermal effect in liquid crystal networks: a general approach for self-sustained mechanical oscillators. Adv. Mater. *29*, 1606712.
3. Jan Mulder, D., Selinger, R.L.B., Konya, A., Gelebart, A.H., Varga, M., Vantomme, G., Meijer, E.W., and Broer, D.J. (2017). Making waves in a photoactive polymer film. Nature *546*, 632–636.
4. Maeda, S., Hara, Y., Sakai, T., Yoshida, R., and Hashimoto, S. (2007). Self-walking gel. Adv. Mater. *19*, 3480–3484.
5. Kim, Y.S., Tamate, R., Akimoto, A.M., and Yoshida, R. (2017). Recent developments in self-oscillating polymeric systems as smart materials: from polymers to bulk hydrogels. Mater. Horizons *4*, 38–54.
6. Ren, L., She, W., Gao, Q., Pan, C., Ji, C., and Epstein, I.R. (2016). Retrograde and direct wave locomotion in a photosensitive self-oscillating gel. Angew. Chem. Int. Ed. *55*, 14301–14305.
7. Yoshida, R. (2010). Self-oscillating gels driven by the Belousov-Zhabotinsky reaction as novel smart materials. Adv. Mater. *22*, 3463–3483.
8. Tamate, R., Mizutani Akimoto, A., and Yoshida, R. (2016). Recent advances in self-oscillating polymer material systems. Chem. Rec. *16*, 1852–1867.
9. Zhao, Y., Xuan, C., Qian, X., Alsaid, Y., Hua, M., Jin, L., and He, X. (2019). Soft phototactic swimmer based on self-sustained hydrogel oscillator. Sci. Robot. *4*, eaax7112.
10. Yashin, V.V., and Balazs, A.C. (2006). Pattern formation and shape changes in self-oscillating polymer gels. Science *314*, 798–802.
11. Elices, I., Levi, R., Arroyo, D., Rodriguez, F.B., and Varona, P. (2019). Robust dynamical invariants in sequential neural activity. Sci. Rep. *9*, 1–13.
12. Del Negro, C.A., Funk, G.D., and Feldman, J.L. (2018). Breathing matters. Nat. Rev. Neurosci. *19*, 351–367.
13. Yoshida, R., Takahashi, T., Yamaguchi, T., and Ichijo, H. (1996). Self-oscillating gel. J. Am. Chem. Soc. *118*, 5134–5135.
14. Murase, Y., Maeda, S., Hashimoto, S., and Yoshida, R. (2009). Design of a mass transport surface utilizing peristaltic motion of a self-oscillating gel. Langmuir *25*, 483–489.
15. Vanag, V.K., and Epstein, I.R. (2001). Inwardly rotating spiral waves in a reaction-diffusion system. Science *294*, 835–837.
16. Petrov, V., Gáspár, V., Masere, J., and Showalter, K. (1993). Controlling chaos in the Belousov—Zhabotinsky reaction.. Nature (Nature Publishing Group), pp. 240–243. http://www.nature.com/articles/361240a0.
17. Semenov, S.N., Kraft, L.J., Ainla, A., Zhao, M., Baghbanzadeh, M., Campbell, V.E., Kang, K., Fox, J.M., and Whitesides, G.M. (2016). Autocatalytic, bistable, oscillatory networks of biologically relevant organic reactions. Nature *537*, 656–660.
18. Semenov, S.N., Wong, A.S.Y., Van Der Made, R.M., Postma, S.G.J., Groen, J., Van Roekel, H.W.H., De Greef, T.F.A., and Huck, W.T.S. (2015). Rational design of functional and tunable oscillating enzymatic networks. Nat. Chem. *7*, 160–165.
19. Qian, X., Zhao, Y., Alsaid, Y., Wang, X., Hua, M., Galy, T., Gopalakrishna, H., Yang, Y., Cui, J., Liu, N., et al. (2019). Artificial phototropism for omnidirectional tracking and harvesting of light. Nat. Nanotechnol. *14*, 1048–1055.
20. Jiang, R., Xiao, J., and Song, J. (2017). Buckling of thin gel strip under swelling. Theor. Appl. Mech. Lett. *7*, 134–137.
21. Kang, S.H., Shan, S., Košmrlj, A., Noorduin, W.L., Shian, S., Weaver, J.C., Clarke, D.R., and Bertoldi, K. (2014). Complex ordered patterns in mechanical instability induced geometrically frustrated triangular cellular structures. Phys. Rev. Lett. *112*, 098701.
22. Kang, S.H., Shan, S., Noorduin, W.L., Khan, M., Aizenberg, J., and Bertoldi, K. (2013). Buckling-induced reversible symmetry breaking and amplification of chirality using supported cellular structures. Adv. Mater. *25*, 3380–3385.
23. Rafsanjani, A., Zhang, Y., Liu, B., Rubinstein, S.M., and Bertoldi, K. (2018). Kirigami skins make a simple soft actuator crawl. Sci. Robot. *3*, eaar7555.
24. Rafsanjani, A., Bertoldi, K., and Studart, A.R. (2019). Programming soft robots with flexible mechanical metamaterials. Sci. Robot. *4*, 2–5.
25. Coulais, C., Sabbadini, A., Vink, F., and van Hecke, M. (2018). Multi-step self-guided pathways for shape-changing metamaterials. Nature *561*, 512–515.
26. Rothemund, P., Ainla, A., Belding, L., Preston, D.J., Kurihara, S., Suo, Z., and Whitesides, G.M. (2018). A soft, bistable valve for autonomous control of soft actuators. Sci. Robot. *3*, eaar7986.
27. Preston, D.J., Rothemund, P., Jiang, H.J., Nemitz, M.P., Rawson, J., Suo, Z., and Whitesides, G.M. (2019). Digital logic for soft devices. Proc. Natl. Acad. Sci. U S A *116*, 7750–7759.
28. Korner, K., Kuenstler, A.S., Hayward, R.C., Audoly, B., and Bhattacharya, K. (2020). A nonlinear beam model of photomotile structures. Proc. Natl. Acad. Sci. U S A *117*, 9762–9770.
29. Shin, B., Ha, J., Lee, M., Park, K., Park, G.H., Choi, T.H., Cho, K.J., and Kim, H.Y. (2018). Hygrobot: a self-locomotive ratcheted actuator powered by environmental humidity. Sci. Robot. *3*, 1–9.
30. Arazoe, H., Miyajima, D., Akaike, K., Araoka, F., Sato, E., Hikima, T., Kawamoto, M., and Aida, T. (2016). An autonomous actuator driven by fluctuations in ambient humidity. Nat. Mater. *15*, 1084–1089.
31. Wehner, M., Truby, R.L., Fitzgerald, D.J., Mosadegh, B., Whitesides, G.M., Lewis, J.A., and Wood, R.J. (2016). An integrated design and fabrication strategy for entirely soft, autonomous robots. Nature *536*, 451–455.
32. Shastri, A., McGregor, L.M., Liu, Y., Harris, V., Nan, H., Mujica, M., Vasquez, Y., Bhattacharya, A., Ma, Y., Aizenberg, M., et al. (2015). An aptamer-functionalized chemomechanically modulated biomolecule catch-and-release system. Nat. Chem. *7*, 447–454.
33. He, X., Friedlander, R.S., Zarzar, L.D., and Aizenberg, J. (2013). Chemo-mechanically regulated oscillation of an enzymatic reaction. Chem. Mater. *25*, 521–523.
34. Chen, X., Goodnight, D., Gao, Z., Cavusoglu, A.H., Sabharwal, N., Delay, M., Driks, A., and Sahin, O. (2015). Scaling up nanoscale water-driven energy conversion into evaporation-driven engines and generators. Nat. Commun. *6*, 1–7.
35. White, T.J., and Broer, D.J. (2015). Programmable and adaptive mechanics with liquid crystal polymer networks and elastomers. Nat. Mater. *14*, 1087–1098.
36. He, X., Aizenberg, M., Kuksenok, O., Zarzar, L.D., Shastri, A., Balazs, A.C., and Aizenberg, J. (2012). Synthetic homeostatic materials with chemo-mechano-chemical self-regulation. Nature *487*, 214–218.